Sedimentology and magnetic susceptibility of recent sediments from New Caledonia

HÉLÈNE JADOT & FRÉDÉRIC BOULVAIN*

Pétrologie sédimentaire, B20, Université de Liège, Sart Tilman, B-4000 Liège, Belgium

**Corresponding author (e-mail: fboulvain@ulg.ac.be)*

Abstract: the interpretation of the primary origin of the minerals carrying the magnetic susceptibility (MS) signal from ancient rocks suffers notably from the scarcity of studies on Recent sediments. To bring new data, a study of tropical coastal sediments of New Caledonia was undertaken. This island is surrounded by a nearly uninterrupted reef barrier, isolating a wide lagoon from the open ocean. The erosion of extremely varied rocks (from mantle rocks to laterites) produces different types of detrital sediments, which are mixed with the indigenous precipitated carbonates. This generates different types of coastal sediments, detrital- or carbonate-dominated or mixed. More than 300 samples were analysed for grain size, nature of sediment, MS and geochemistry (major elements). The first results show that: (a) carbonate sands and carbonate silts are characterized by lower MS than detrital sediments; (b) the MS signal of mixed sediments is mostly influenced by the proportion of detrital sediments; (c) MS is directly correlated with Mn and Fe content; (d) beachrocks are characterized by lower MS than equivalent loose sediment; (e) the MS signal of carbonate sediments is locally positively correlated with granulometry; (f) there is no MS change between surface and 20 cm deep samples; and (g) when the subsurface sediment is reducing, the MS is higher than that from surface sediment.

Changes in magnetic susceptibility (MS) of sedimentary successions are considered to be related to sea-level variations (Devleeschouwer 1999; Ellwood *et al.* 1999). This inferred relationship led to the proposal to use MS for high-resolution global correlation of marine sedimentary rocks (e.g. Crick *et al.* 1997). The major influence of sea-level on the MS signal is related to the link between MS and detrital components and the assumption that the detrital input is generally controlled by eustasy (Crick *et al.* 2001). In this way, a sea-level fall increases the proportion of exposed continental area, increases erosion and leads to higher MS values, whereas rising sea-level decreases MS (Crick *et al.* 2001). However, climatic variations influence MS through changes in rainfall (high rainfall increases erosion and MS), glacial–interglacial periods (glacial periods involve glacial erosion together with marine regression and both effects increase MS) and pedogenesis (formation of magnetic minerals in soils: Crick *et al.* 2001). In addition to subaqueous delivery, different authors have considered that magnetic minerals in carbonate sediments can also be supplied from aeolian suspension and atmospheric dust (Hladil 2002; Hladil *et al.* 2006, 2009; Whalen & Day 2008). Furthermore, early and late diagenesis can be responsible for MS variation through mineralogical transformations, dissolution or authigenesis (Rochette 1987; McCabe & Elmore 1989; Zegers *et al.* 2003).

A few studies have proposed a link between MS and depositional environment (Borradaile *et al.* 1993; Da Silva & Boulvain 2006; Da Silva *et al.* 2009*a*, *b*). These studies presented different MS/depositional environment responses in different platform types, suggesting that sea-level changes leading to variation in detrital input is not the only parameter controlling average MS values. Other primary or secondary processes probably also influenced magnetic mineral distribution. Primary processes such as water agitation and carbonate production during deposition seem to be important factors (Da Silva *et al.* 2009*b*).

MS studies of ancient sediments are now relatively common, for example, Lower Palaeozoic: Debacker *et al.* (2010); Lower Devonian: Koptíková *et al.* (2010), Hladil *et al.* (2010), Vacek (2011); Middle Devonian: Mabille & Boulvain (2007), Boulvain *et al.* (2010); Upper Devonian: Da Silva *et al.* (2009*b*); Da Silva & Boulvain (2012); Mississippian: Bábek *et al.* (2013), Bertola *et al.* (2013); Triassic: Spahn *et al.* (2013), Michalík *et al.* (2013); Jurassic: Boulila *et al.* (2008); Cretaceous: Grabowski & Pszczo1kowski (2006); Cenozoic: Donghuai *et al.* (1998). MS studies are also a prerequisite for Quaternary sedimentary research, in marine and continental settings, for example, Bloemendal *et al.* (1988), Bender *et al.* (2012), Hladil *et al.* (2003), Tang *et al.* (2003). Surprisingly, however, very few studies are dedicated to present-day littoral sediments (McNeill *et al.* 1988; Hladil *et al.* 2003, 2004).

This study applies magnetic susceptibility measurements to recent tropical carbonate, detrital and mixed littoral sediments. In view of the lack

From: Da Silva, A. C., Whalen, M. T., Hladil, J., Chadimova, L., Chen, D., Spassov, S., Boulvain, F. & Devleeschouwer, X. (eds) *Magnetic Susceptibility Application: A Window onto Ancient Environments and Climatic Variations*. Geological Society, London, Special Publications, **414**, http://dx.doi.org/10.1144/SP414.2

of studies on present-day littoral sediments and because of unresolved questions about the impact of various external parameters on the MS signal, the main goals of this paper are as follows: (a) to document the link between MS and different active environmental parameters such as water agitation during deposition, detrital inputs and carbonate production on a present day carbonate platform; and (b) to check the persistence of the signal in subsurface and to compare it with equivalent surface sediment. For this purpose, New Caledonia was selected, as this tropical island is characterized by highly diversified littoral sediment, ranging from pure carbonate to pure siliciclastic and even to iron oxide-rich sediment.

Methods

From July to September 2012, 22 beaches were sampled along topographic profiles established with a laser level and a measuring tape. Three-hundred samples of loose sediment were taken at the surface and at 10 or 20 cm depth, together with five blocks from beachrocks and hardgrounds. The MS measurements were made on a KLY-3 Kappabridge device (cf. Da Silva & Boulvain 2006). Three measurements were made on each sample weighed with a precision of 0.01 g. Every sample was observed under binocular microscope to evaluate the proportion of the different types of grains. For better grain identification, petrographic analyses were made on thin sections from resin-indurated sediment. Grain-size analyses were performed on a 1 mm wire screen for the coarse fraction of the sediments and with a Malvern Mastersizer 2000 laser granulometer for the <1 mm fraction of carbonate sediments. The amount of sediment was selected to obtain a laser obscuration rate of 10–20%. Major element geochemistry was completed using X-ray fluorescence (ARL 9400 XP XRF instrument, University of Liège). One sample per beach was crushed with a Bauknecht crusher and milled in agate mortars. The total concentrations of major elements were measured on lithium tetra- and metaborate fused glass discs, with matrix corrections following the TrailleLachance algorithm and are expressed as oxide concentrations. Accuracy is estimated as better than 1% for major elements as checked with 40 international and in-house standards.

General setting

Geographical, structural and geological settings

New Caledonia is an island located 1500 km East of Australia, in the Coral Sea (SW Pacific Ocean). The main island, called Grande Terre, is situated between the Tropic of Capricorn and the eighteenth parallel South and between longitudes 160 and 170°E. Several smaller islands surround the main island (Figs 1a & 2). Grande Terre ranges over 400 km along a NW–SE direction and is prolonged by the Belep islands to the north and the Pins island to the south. The Loyalty archipelago parallels Grande Terre to the east. New Caledonia is surrounded by a vast reef barrier isolating a shallow lagoon, dotted with thousands of islets. Two deep sedimentary basins border New Caledonia: to the west, the New Caledonia basin reaches 3500 m deep, and to the east, the Loyalty basin is slightly shallower (2000–3000 m). Further to the east, the New Hebrides trench corresponds to an active subduction zone (Dupont & Daniel 1981; Lambert & Roux 1991; Fig. 1b). A mountain range encompassing several peaks over 1000 m in height separates two coastal area with different characteristics (Paris 1981): the eastern coast of Grande Terre has

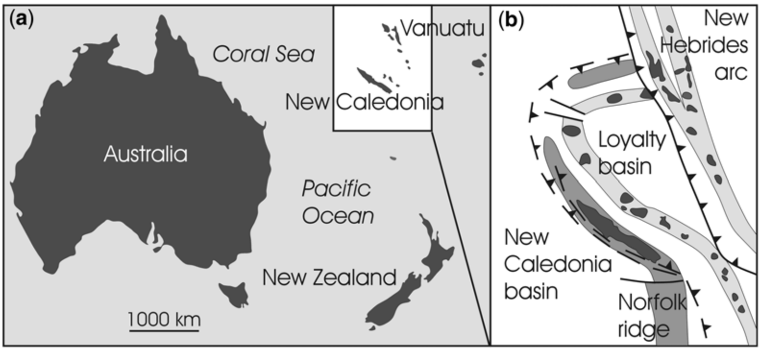

Fig. 1. (**a**) Location of New Caledonia in the Southwestern Pacific ocean. (**b**) Major structural features of the Southwestern Pacific ocean. After Cluzel (2006).

a hilly relief with steep inclines and cliffs along the ocean, while the western coast is made up of swampy lowlands with large alluvial plains.

Structurally, New Caledonia corresponds to the emerged northern part of the Norfolk ridge, ending in New Zealand (Fig. 1b). This granitic ridge is located between Australia and the active New Hebrides island arc, marking the limit between the Indo-Australian and Pacific plates. New Caledonia separated from Australia at the end of Cretaceous (Cluzel 2006).

The oldest Caledonian rocks are of Carboniferous age. The Carboniferous–Cretaceous sedimentary basement is covered by the Poya basaltic thrust sheet, itself covered during the Eocene by obducted peridotites (Cluzel *et al.* 2012). The Carboniferous–Cretaceous basement consists of three subparallel units in the central part of the island: the Koh–Chaîne Centrale unit, the Boghen unit and the Teremba unit (Fig. 2). In the northern part of Grande Terre, three other younger units unconformably overlie the former ones: the Montagne Blanche, Diahot and Pouébo units (Cluzel 2006; Cluzel *et al.* 2012; Audet 2008).

- The Koh–Chaîne Centrale unit corresponds to a part of the oceanic floor: Carboniferous ophiolites are topped by volcaniclastic formations of Upper Triassic to Lower Jurassic age.
- The Boghen unit is made up of Jurassic to Cretaceous basaltic and volcaniclastic rocks, metamorphosed to green-schist grade.
- The Teremba unit consists of fossil-rich volcano-sedimentary rocks dated from Upper Permian to Middle Jurassic.
- The Montagne Blanche unit is rich in carbonates and detrital sediments and is dated from the Upper Cretaceous.
- The Diahot unit is made up of Upper Cretaceous volcaniclastic rocks with a blue-schist grade metamorphism.
- The Pouébo unit is similar to the Diahot unit, but shows a metamorphism of the eclogite grade.

The peridotitic thrust sheet, largely cropping out in the southern part of Grande Terre, is topped by a well-developed, several tens of metres-thick, iron-rich duricrust dated as Miocene in age (Audet 2008; Tercinier 1962). The Loyalty islands and part of the

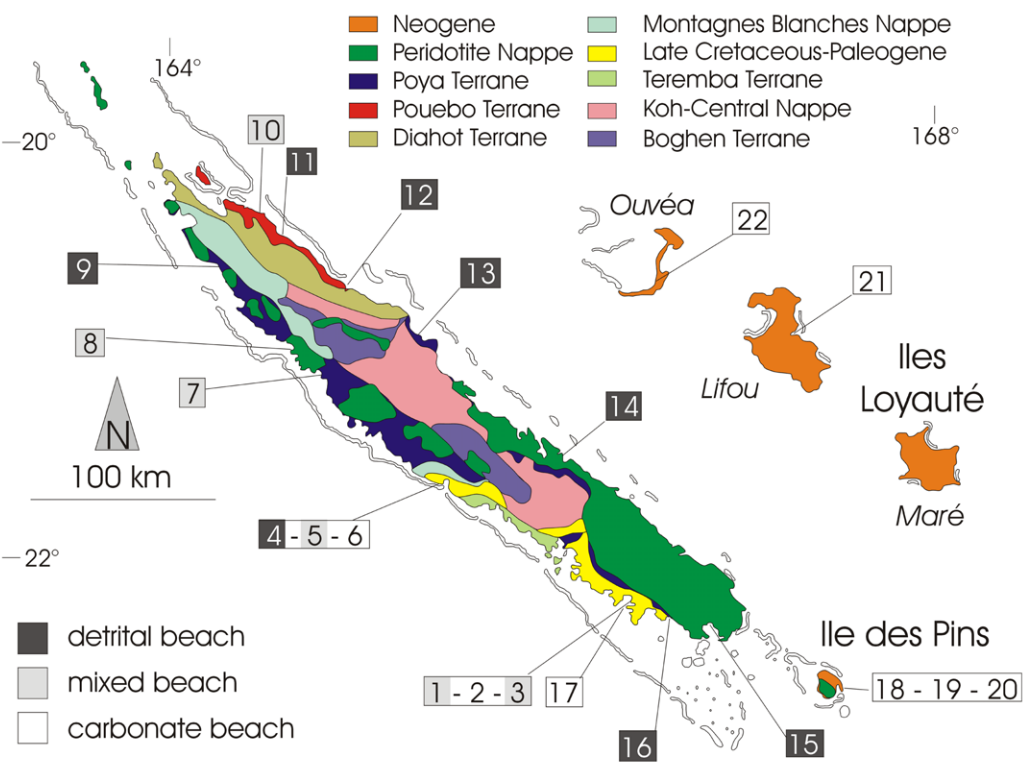

Fig. 2. Simplified geological map of New Caledonia and Loyalty Islands. After Cluzel *et al.* (2012). Location of the sampled beaches, cf. Table 1.

eastern coast of Grande Terre were uplifted during the Neogene as a result of the lithospheric flexure related to the New Hebrides subduction zone (Lambert & Roux 1991).

Climate and hydrology

New Caledonia benefits from a tropical climate, with alternating dry and wet seasons. During the austral winter, the island is situated under the subtropical high-pressure belt and the easterly trade winds. During the summer, the equatorial lows generate westerly winds and typhoons (Lambert & Roux 1991; Ouillon *et al.* 2010). The eastern coast is more affected by wind and is rainier than the western coast. Rainfall in Nouméa (south of Grande Terre) averages 1100 mm a^{-1} with a maximum in February. Many torrents and rivers drain Grande Terre and provide detrital sediments to the lagoon, especially after tropical storms, during which sediment load may reach 0.5 g l^{-1} (Baltzer & Trescases 1971). However, chemical erosion is pre-eminent, with a loss of material of 27 mm a^{-1}, while mechanical erosion has been evaluated as close to 11 mm a^{-1} (Baltzer & Trescases 1971).

Sedimentology

In New Caledonia, the maximum tidal range is close to 1.7 m; however, during storm surges, the lowlands of the western coast are flooded (Baltzer & Trescases 1971). Ocean currents flow from SE along the eastern coast of New Caledonia and from NW along the western coast. The carbonate platform surrounding New Caledonia started to build at the beginning of Miocene (Montaggioni *et al.* 2011). Its development was largely controlled by eustacy and tectonism and, locally, its thickness reaches 200 m. Before the onset of the barrier reef system near 0.4 Ma (MIS 11), carbonate sediment accumulated on a ramp (Montaggioni *et al.* 2011). Nowadays, the barrier is less continuous along the eastern coast of New Caledonia than along its western coast, where it is only interrupted by some channels (Chevillon 1997; Ouillon *et al.* 2010). The reef barrier is made up of corals, coralline algae and sponges (Clavier & Garrigue 1999). Two main communities are distinguished: a *Porites*-dominated community, with massive coral morphologies; and an *Acropora*-dominated community with branching forms (Montaggioni *et al.* 2011). The barrier protects the lagoon from ocean swell.

The lagoon is 5–40 km wide and is very shallow. The widest lagoon is located along the southwestern coast of Grande Terre. Actually, the lagoon of New Caledonia has been well studied for biological, sedimentological and environmental protection purposes (Chevillon 1997; Grenz *et al.* 2010; Ouillon *et al.* 2010). Given the small size of inland watersheds, the fresh-water supply to the lagoon is low and of the same order as the oceanic inward and outward currents (Ouillon *et al.* 2010). The detrital sediment supply by rivers is effective only during flood periods while, during rough sea, the transfer of carbonate sediment from the barrier to the lagoon is active (Ouillon *et al.* 2010). Lagoonal sediments are categorized in three facies according their grain size: (a) 0.25–0.5 mm; (b) *c.* 0.125 mm; and (c) <63 μm. Facies (a) and (c) are observed everywhere in the lagoon; ashore and close to the river mouths, facies (a) is missing and there is a balance between facies (b) and (c) and finally, close to the barrier, facies (b) dominates (Ouillon *et al.* 2010). Foraminifers and molluscs are the major contributors to the carbonate fraction of the sediment, together with corals and algae close to the barrier. Detrital sediment coming from rivers is more concentrated in stock (c). Detailed studies of the eastern lagoon by Chevillon (1997) and of the southwestern lagoon by Dugas & Debenay (1980) and Chevillon (2013) show a grain size decrease from the back barrier area to the beach, together with a concentration of detrital sediments along the shore and of carbonates along the barrier.

Ashore, an uninterrupted 100–300 m-wide fringing reef develops all along the eastern coast. Some fringing reefs are also observed along the western coast, but they are local (Lambert & Roux 1991).

Results

Twenty-two beaches were sampled, all around Grande Terre and on the Pins, Lifou and Ouvéa islands (Fig. 2). All of the profiles studied are perpendicular to the beaches and extend from the sea to the supratidal zone. In New Caledonia, this zone is covered with rich tropical vegetation or with grass. The seaward edge of the supratidal zone corresponds to a microcliff when eroded by storm waves or to a sandy berm when sediment accumulation outpaces erosion. The intertidal zone is relatively narrow (7–35 m wide, cf. Table 1), probably because of low tidal range and minor swell. Mangrove develops locally (Virly 2008; Marchand *et al.* 2010), as well as beachrocks or reef flats when a fringing reef is present. With the exception of this last case, sediments are relatively fine-grained, except close to river mouths where a large range of detrital sediments are mixed with autochthonous carbonates (Chevillon 1997). The boundary between intertidal and subtidal zones is commonly covered by turtle grass (*Thalassia*) (Chevillon 2013) and marks the end of the profiles.

Table 1. *Number, name, location and main characteristics of the profiles*

	Name	Nearest city or village	Coordinates	↔ (m)	↕ (m)	Number of samples
1	Anse de Kuendu	Nouméa	22°15′37.6″S/166°23′24.7″E	35	1.85	17
2	Kuendu 2	Nouméa	22°15′35.7″S/166°23′15.5″E	7.5	1.81	9
3	Kuendu 3	Nouméa	22°15′41.5″S/166°23′19.6″E	10	1.83	12
4	Roche Percée	Bourail	21°36′29.9″S/165°27″34.5″E	35	3.05	18
5	Baie des Tortues	Bourail	21°36′22.7″S/165°27′15.4″E	23	4.14	16
6	Poé	Bourail	21°36′47.2″S/165°23′59.3″E	12.3	1.86	19
7	Foué	Koné	21°05′58.8″S/164°49′25.7″E	10	0.72	16
8	Gatope	Voh	20°58′02.8″S/164°39′27.9″E	8.7	1.12	14
9	Pointe de Pandope	Koumac	20°34′19.0″S/164°16′35.9″E	5.7	0.6	10
10	Maamat	Pouébo	20°17′43.3″S/164°25′53.9″E	11.1	1.12	14
11	Pouébo	Pouébo	20°29′31.1″S/164°45′04.8″E	10	1.13	19
12	Hienghène	Hienghène	20°41′15.3″S/164°56′47.7″E	14.5	0.76	18
13	Poindimié	Poindimié	20°53′42.1″S/164°19′14.3″E	13.5	2.04	18
14	Plage de Ouroué	Thio	20°53′42.1″S/165°19′14.3″E	9.2	0.88	12
15	Prony	Prony	22°19′37.3″S/166°49′22.6″E	3	0.64	7
16	Plum	Mont Dore	22°17′06.0″S/166°38′43.3″E	7.5	0.88	11
17	Ilot Maitre	Nouméa	22°20′06.6″S/166°24′35.1″E	9.5	1.5	14
18	Baie de Kuto	Ile des Pins (Kunie)	22°39′13.7″S/167°26′30.3′ E	19.7	2.44	18
19	Baie de Ouaméo	Ile des Pins (Koojë)	22°35′19.4″S/167°25′29.5″E	12	1.41	14
20	Baie d'Upi	Ile des Pins (Vao)	22°36′04.9″S/167°31′31.8″E	6	0.38	11
21	Baie de Chateaubriand	Lifou (Wé)	20°54′22.7″S/167°15′24.7″E	25.9	2.24	26
22	Baie de Wadrilla	Ouvéa (Fayaoué)	20°38′04.2″S/166°32′46.5″E	9.7	1.29	14

Carbonate beaches are in roman, detrital beaches in *italics* and mixed ones in **bold**.

The beaches

The main characteristics of the sediments and of the beaches selected for sampling are listed below and are synthesized in Tables 2–4. Figure 3 shows some characteristic topographic profiles.

- *Anse de Kuendu* (1): this beach is located at the bottom of a small bay on the Nou peninsula, close to Nouméa. Cliffs with cherty beds circumscribe the bay, but no river flows into it. Kuendu bay is relatively protected from winds and currents and a fringing reef develops as well as along the southern shore of the peninsula. On this relatively gentle profile, bioclasts are slightly dominant over lithoclasts and the upper intertidal zone is characterized by a high water mark made from coral gravel. Seaward, the coarse sand (1–2 mm in size) passes progressively to a finer sand.
- *Kuendu* 2 (2): this well-exposed beach is characterized by more bioclasts than the former one. Gravels are abundant and sands are present only along the seaward end of the profile.
- *Kuendu* 3 (3): this site is bounded by a cliff. Sediments consist of bioclastic and lithoclastic gravels.
- *Roche Percée* (4): the Roche Percée beach is a sand bank situated at the mouth of the Nera river. It faces a channel in the reef barrier and is sometimes affected by storm waves. The grey sand is very well sorted and dominated by detrital grains supplied by the river.
- *Baie des Tortues* (5): close to the former site, this relatively steep beach (Fig. 3) is delimited by cliffs of siliciclastic turbidites (Cluzel *et al.* 2012). However, the coarse sand and gravel (1–3 mm) are dominated by bioclasts.
- *Poé* (6): this narrow beach is protected by an adjacent reef barrier (<1 km), and sufficiently far from the Nera mouth to consist of nearly pure carbonate fine sand and silt. Locally, a beachrock develops. The lagoon is particularly shallow (*c.* 1 m).
- *Foué* (7): Foué is situated some 10 km from Koné, a city on the western coast of Grande Terre. This area is characterized by basalts of the Poya unit. The grey fine sands of this relatively protected beach are of mixed origin. No river flows in the vicinity of the beach and detrital sediments are supposed to be delivered by longshore marine currents.
- *Gatope* (8): the Gatope peninsula is close to the Voh village, along the northwestern coast of Grande Terre. In this area, mangroves flourish in the river mouths. The beach is relatively protected from fluvial detrital supply and lithoclasts originate through the marine erosion of basaltic

Table 2. *Microscope estimation of sediment composition by beaches*

	Name	Lithoclasts (%)	Bioclasts (%)	Micritic grains	Bivalves	Gastropods	Corals	Foraminifers	Algae	Sponge spicules	Bryozoans
1	Anse de Kuendu	40	60	++	+	+	+	o	+	o	o
2	Kuendu 2	15	85	–	o	o	+++	\	\	\	\
3	Kuendu 3	15	85	+	+	+	+++	o	\	o	\
4	Roche Percée	60–70	30–40	++	+	+	+	+	\	\	\
5	Baie des Tortues	30	70	++	++	++	++	++	o	o	o
6	Poé	<5	95	+++	+	+	+	+	+	o	o
7	Foué	40	60	+	++	++	++	o	+	\	\
8	Gatope	60	40	+	+	+	o	\	\	\	o
9	Pointe de Pandope	70	30	\	++	++	\	\	\	\	\
10	Maamat	70	30	o	++	+	++	+	\	o	o
11	Pouébo	90	10	\	+	+	+	–	\	\	\
12	Hienghène	85–90	10–15	+	+	+	+	+	\	\	\
13	Poindimié	65–70	30–35	++	+	+	+	o	\	\	\
14	Plage de Ouroué	90	10	+	+	+	\	\	\	\	\
15	Prony	80–85	15–20	+	+	+	+	\	\	\	\
16	Plum	75	25	++	++	+	o	o	–	\	\
17	Ilot Maitre	\	100	++	++	++	+++	++	o	o	\
18	Baie de Kuto	2	98	+++	++	++	++	++	o	+	o
19	Baie de Ouaméo	1	99	++	++	++	++	++	+	+	o
20	Baie d'Upi	\	100	++	++	+++	+	+	+	o	o
21	Baie de Chateaubriand	2–3	97–98	+++	+	+	+++	+	+	++	o
22	Baie de Wadrilla	1–2	98–99	+	+++	+++	++	+	++	+	o

+++ = abundant; ++ = frequent; + = present; o = rare; − = very rare (fewer than five grains observed in all the samples of a beach); \ = absent. Carbonate beaches are in roman, detrital beaches in *italics* and mixed ones in **bold**.

Table 3. *Average proportion of gravel and sand for detrital and mixed beaches*

	Name	Percentage gravel (>5 cm)	Percentage gravel (<5 cm)	Percentage sand
1	Anse de Kuendu	10	10–20	60–70
2	Kuendu 2	45	45	10
3	Kuendu 3	30	40	30
4	Roche Percée	1	5	94
5	Baie des Tortues	\	\	100
7	Foué	5	30	65
8	Gatope	\	2	98
9	Pointe de Pandope	5	60	45
10	Maamat	5	45	50
11	Pouébo	5	30	65
12	Hienghène	\	2	98
13	Poindimié	\	5	95
14	Plage de Ouroué	\	2	98
15	Prony	\	15	85
16	Plum	\	10	90

Carbonate beaches are in roman, detrital beaches in *italics* and mixed ones in **bold**.

outcrops of the Poya unit. The grey sand is mixed and poorly rounded.

- *Pointe de Pandope* (9): this is a peninsula close to the town of Koumac, one of the main cities in the North of New Caledonia. The beach is situated close to the mouth of the Koumac river, where mangrove grows. The sediment is very coarse and gravels are derived from close outcrops of flysch, sandstone and basalt.
- *Maamat* (10): this beach is located along the northeastern coast of Grande Terre and is protected by a close reef barrier. No river is present, but quartz gravels are observed and the fine sand is rich in micas, probably coming from outcrops of high-grade metamorphic rocks. Corals debris, coquinas and quartz cobbles are present.
- *Pouébo* (11): this beach is located in the same geological context as the former. Quartz gravel and micas are abundant but bioclasts are scarcer. A beachrock is observed and a fringing reef parallels the shore.
- *Hienghène* (12): this gentle beach (Fig. 4a) is located in Hienghène bay, close to the eponymous river mouth. Eocene limestone outcrops supply a noticeable fraction of the sand. A fringing reef develops, except in the river mouth.
- *Poindimié* (13): the Poindimié area is characterized by basaltic rocks from the Poya unit. This relatively steep sandy–silty detrital beach is close to a little stream. A fringing reef is locally present and high-water marks rich in coquina are observed.
- *Plage de Ouroué* (14): the Ouroué beach next to the village of Thio is located close to weathered outcrops of peridotites and basalts. The nearby Thio river brings varied detrital material to the beach and the well-sorted sands that mainly consist of lithoclasts of laterite.

Table 4. *Detailed grain size data for carbonate sediments*

	Name	Gravel % (>5 cm)	Gravel % (<5 cm)	Sand %	Silt %	Finest grains % (<2 μm)	Median (μm)	Mean (μm)	Sorting	Skewness	Kurtosis
6	Poé	\	5	94.2	0.69	0.11	439	464	0.67	0.06	1
17	Ilot Maitre	\	\	97.7	2.13	0.16	742	777	0.73	0.11	1.32
18	Baie de Kuto	\	5	94.8	0.25	0	209	222	0.61	−0.02	0.99
19	Baie de Ouaméo	\	2	96.55	1.44	0.01	364	392	0.75	0.07	0.99
20	Baie d'Upi	\	5	71.20	22.68	1.11	236	262	1.52	0.29	1.36
21	Baie de Chateaubriand	\	\	99.6	0.40	0.00	308	343	0.74	−0.02	0.95
22	Baie de Wadrilla	5	3	64.89	10.00	0.00	382	412	0.69	−0.02	0.94

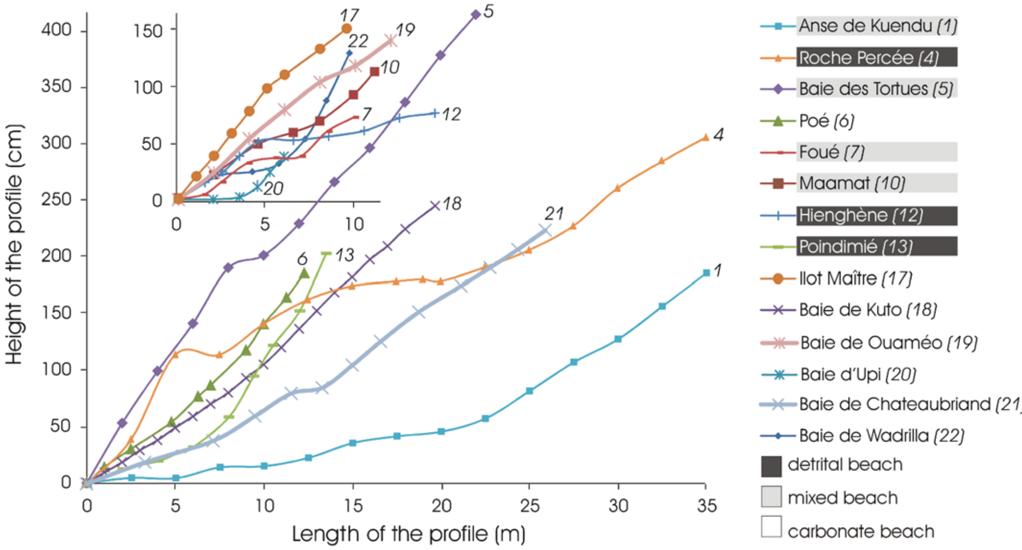

Fig. 3. Topographic profiles and location of samples for some characteristic beaches.

- *Prony* (15): this village is situated close to the south end of Grande Terre. The sampling was performed in a relatively protected area called Baie de la Somme, where many little creeks carrying lateritic material end. The intertidal zone is steep and narrow, covered by coarse reddish detrital sand. Some grains are bioclasts coated by iron oxides.
- *Plum* (16): the Carcassonne beach is located at the south end of the Mont Dore bay and is 1 km from the mouth of the Pirogues river, bringing large quantities of lateritic material. However, a bioclastic fraction is present and high-water marks rich in bivalves are frequent. The sediment consists of fine sand and gravels.
- *Ilot Maître* (17): this small island is 4 km from Nouméa and at an equal distance from the reef barrier. Its northwestern coast is narrow and exposes hardgrounds and beachrocks, while the southeastern beach is broader and characterized by coarse bioclastic sand and gravel. A fringing reef develops all around the island.
- *Baie de Kuto* (18): the central part of the Pins Island corresponds to weathered peridotites, surrounded by an uplifted fringing reef. A new fringing reef is currently developing all around the island, except in the sheltered bays. Southwest of the Pins island, the Baie de Kuto is a 1 km-long beach, protected from winds. Some outcrops of limestone are observed. The

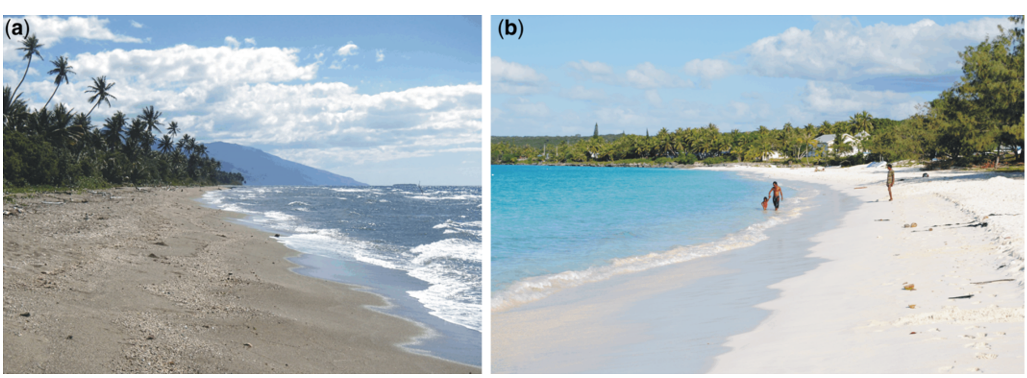

Fig. 4. (**a**) A detritic quartz-rich beach near Hienghène (12) and (**b**) a carbonate beach (Baie de Chateaubriand) in Lifou (21).

sediment consists of fine sand and coral–bivalve–algae gravels.

- *Baie de Ouaméo* (19): this bay, located along the northwestern coast of the Pins island, is characterized by coarser carbonate sediment than the former. This coarser sand consists of foraminifers, algae, corals and bivalves bioclasts. It expands underwater and is covered by turtle grass before giving way to a fringing reef.
- *Baie d'Upi* (20): this very restricted bay is located in the northwestern part of the Pins island. The sediment is relatively fine-grained and the intertidal zone shows an upper bioclastic sandy part and a lower silty part, covering an old fringing reef. Further into the subtidal zone, coarser sand is present again, locally colonized by algae. The limit between the intertidal and supratidal zones is marked by an accumulation of coquina and plant debris.
- *Baie de Chateaubriand* (21): this bay is situated in the northeastern part of the Lifou Island (Loyautés archipelago) (Fig. 4b). This island, surrounded by a fringing reef, is framed by an uplifted Neogene reef and made up entirely of carbonates. The bioclastic sand ends in the subtidal zone and pass to the reef. The base of the supratidal zone is delineated by a small erosion cliff, showing layers of pumice (Fig. 14a), probably coming from the New Hebrides volcanoes.
- *Baie de Wadrilla* (22): situated on the Ouvéa island (Loyautés archipelago), the southern part of which being uplifted by the Neogene event, the bay faces the lagoon. The beach is relatively steep and shows a clear slope increase near the limit between the intertidal and supratidal zones. The sand includes some big coquinas and extends into the subtidal zone.

The beachrocks

Beachrocks are cemented beach sediments, frequent in warm climates and water supersaturated with carbonates, causing the development of aragonitic fibrous and micritic Mg-calcite cements (Purser 1980). They are mainly characterized by meniscus and pendant cements. From the five hard rocks sampled on the beaches, three show a close similarity with the loose sediment (same grain size and composition) and beachrock specific cements: the Poé (6) rock shows micritic to microsparitic meniscus cement; the Foué (7) rock is characterized by a micritic pendant cement and the Ilot Maître (17) rock by a fibrous isopachous cement, although closer to a hardground than to a beachrock. The Pouébo (11) and Poindimié (13) rocks correspond to micritized coral colonies with adjacent cemented sediment.

Sediment composition and grain size

Binocular magnifier and polarizing microscope observations allowed identification of the different constituents of the sediments (Table 2). Reworked fragments of rocks (sandstone, basalts, alterites,

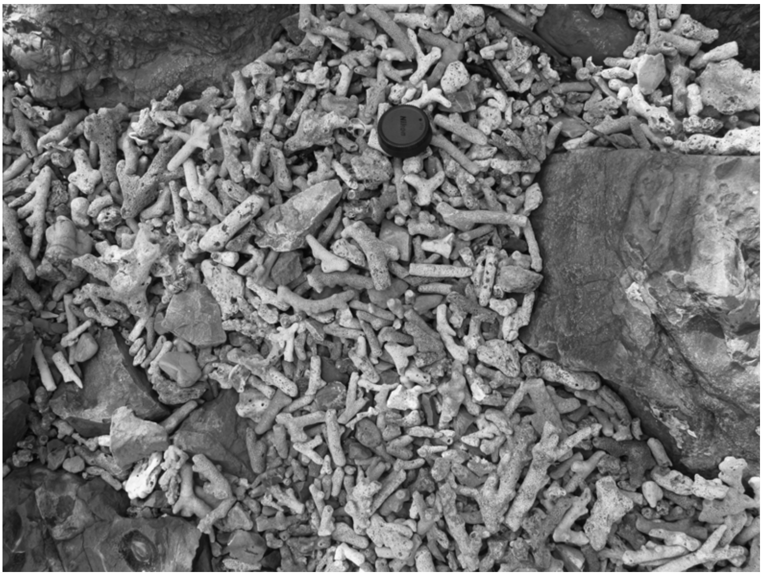

Fig. 5. Coral gravel at Kuendu beach (2).

carbonates, etc.) are classified as lithoclasts. They generally reflect the regional geology. Bioclasts include all fragments of tests, skeletal pieces (Fig. 5), that is, coquina of carbonate-secreting organisms. They also include micritic grains or peletoids *sensu* Blatt *et al.* (1972), which are 50–500 µm angular or rounded pieces of dark micrite, with or without internal structures. These grains are most probably derived from the micritization of bioclasts (Illing 1954; Purser 1980), frequently observed on reef flats. Key bioclasts include bivalves, gastropods, echinoderms, corals, algae, bryozoans and foraminifers. Because of the fine grain size, only algae and foraminifers are easily identifiable. The calcareous chlorophyta *Halimeda* dominates algae and the miliolitid *Marginopora* is the most frequent foraminifer. Other foraminifers like *Elphidium*, together with globigerinids, trilocu-linids and quincoculinids, are also observed (Debenay 2013), as well as the endemic hyaline foraminifer *Hoeglundina*. Some spicules are present and originate from hyaline sponges. Table 2 shows that all carbonate and mixed sediments grossly share the same assemblage, with local differences in the proportions of the different groups.

The grain size was first estimated visually for all of the sediments (Table 3, Fig. 6), then an additional analysis with a laser granulometer was performed on sediments from carbonate beaches because a more developed fine-grained fraction was noticed (Table 4). Generally, every beach has a relatively homogeneous granulometry, with the exception of Kuendu (2) and (3), where sand and gravels cover separated area and Baie d'Upi (20), where sand is replaced by silt in the lower intertidal zone. More specifically, the Kuendu (1–3), Pointe de Pandope (9) and Maamat (10) (Fig. 6d) beaches are characterized by a high proportion of gravel. These beaches are mixed or detrital, or even carbonate (Kuendu 2). The presence of gravel may be related to detrital supply and high flow turbulence (lithoclasts) and/or to the export of bioclasts from a close reef. The Foué (7), Gatope (8), Pouébo (11), Plum (16) and Prony (15) beaches show an enrichment in coarser grains at depth. The Hienghène (12), Plage de Ouroué (14) (Fig. 6c), Baie de Kuto (18) and Baie

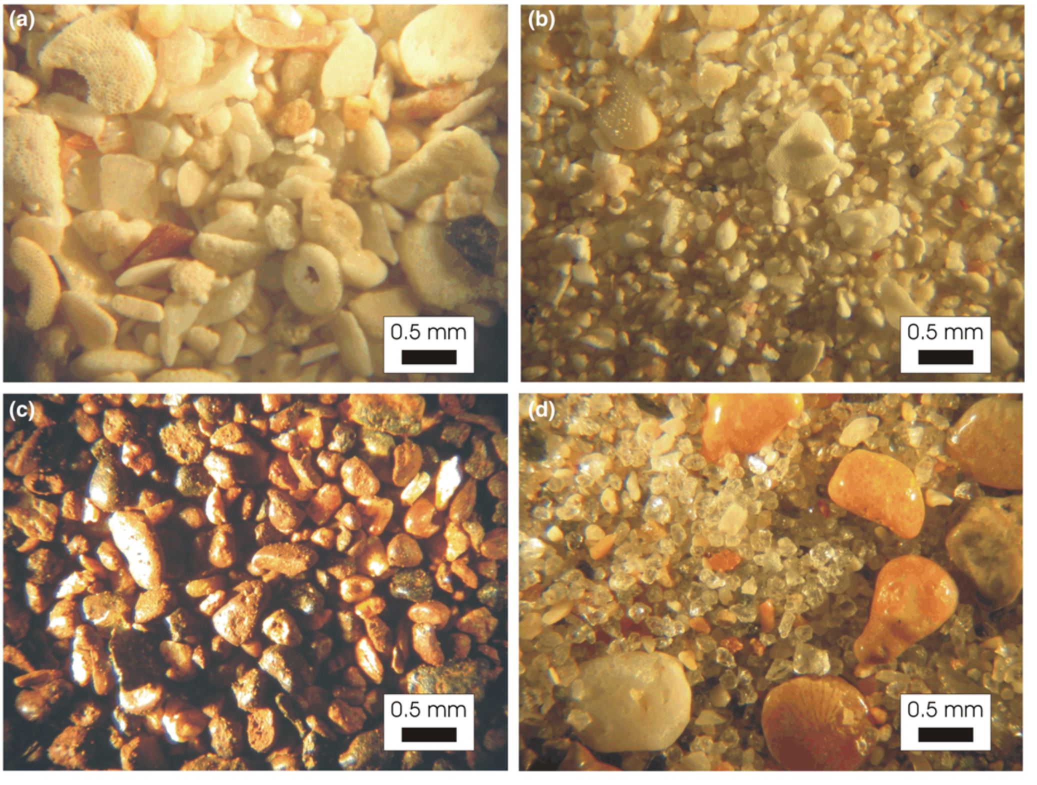

Fig. 6. Examples of carbonate sands: (**a**) Baie de Ouaméo (19), (**b**) Baie de Chateaubriand (21); detrital sand: (**c**) Plage de Ouroué (14); and mixed sand: (**d**) Maamat (10).

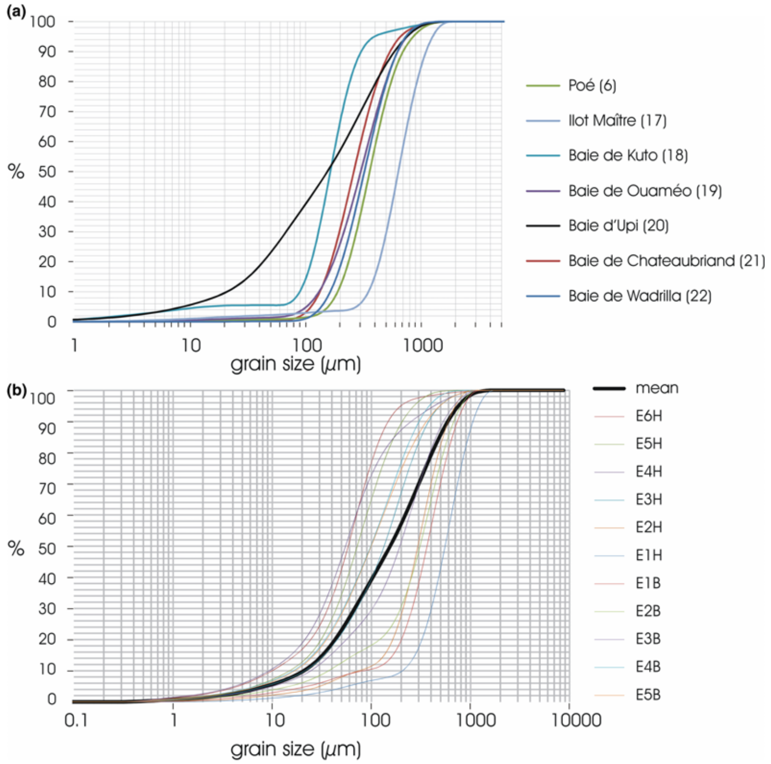

Fig. 7. (**a**) Cumulative granulometric curves for carbonate beaches. For each beach, the curve is the average of all individual curves (arithmetic sum of all different size classes), in order to estimate a global tendency. (**b**) Cumulative granulometric curves for Baie d'Upi (20). H = surface; B = 10 cm deep. Sampling starts in the supratidal zone (E1H) and ends close to the mean tide level (E6H).

de Chateaubriand (21) (Fig. 6b) beaches show fine-grained sediments, except where high-water marks have been sampled. Figure 7a presents the different average cumulative granulometric curves for the carbonate beaches. The analysis of the granulometric curves, using the parameters proposed by Folk & Ward (1957) (sorting, skewness and kurtosis), shows that the carbonate sediments are moderately to moderately well sorted and have a symmetrical and meso- to leptokurtic size distribution. The Baie d'Upi (20) is a noticeable exception, but this is related to the large diversity of the individual samples: from coarse storm deposits to fine-grained lagoonal sediments (Fig. 7b).

Major elements

One sample per beach was selected for X-ray fluorescence analysis. This sample was chosen in the middle of the intertidal zone. Table 5 summarizes the results of the geochemical analysis. These results show that the geochemical composition of the sediments from the different beaches is highly diversified. However, it is possible to categorize the beaches into three groups regarding their geochemical nature:

- The *carbonate beaches*, where CaO is higher than or equal to 90% – Poé (6), Ilot Maître (17), Baie de Kuto (18), Baie de Ouaméo (19), Baie d'Upi (20), Baie de Chateaubriand (21) and Baie de Wadrilla (22); MgO varies and may reach 6%. In these carbonate sediments, Mg most probably comes from Mg-calcite secreted by molluscs, echinoderms or foraminifers. The other elements have low content.
- The *mixed beaches*: the SiO_2 and CaO contents are respectively 15–62 and 28–76%. Fe_2O_3 and Al_2O_3 may reach 10%. Actually, Anse de Kuendu (1), Kuendu (3) and Baie des Tortues (5) are relatively rich in bioclasts and have a high content of CaO, while Foué (7), Gatope (8) and Maamat (10) are richer in quartz.
- The *detrital beaches* with low CaO content (0.2–16%) and high SiO_2 (11–90%), Al_2O_3

Table 5. *X-ray fluorescence analysis (wt%) of major elements for one sample per beach (without LOI)*

	Name	SiO_2	TiO_2	Al_2O_3	Fe_2O_3	MnO	MgO	CaO	Na_2O	K_2O	P_2O_5	Total
1	Anse de Kuendu 5B	22.6	0.1	1.1	0.7	0.0	1.8	71.2	0.7	0.1	0.1	98.5
3	Kuendu 3 5B	20.0	0.1	0.7	0.5	0.0	0.8	75.8	0.9	0.1	0.0	98.9
4	Roche Percée 5B	74.6	0.2	3.5	4.1	0.1	6.7	10.2	1.0	0.3	0.0	100.7
5	Baie des Tortues 4B	15.2	0.1	1.0	1.3	0.1	6.9	74.0	0.7	0.1	0.1	99.3
6	Poé 4B	0.6	0.1	0.3	0.3	0.0	4.6	92.0	0.5	0.1	0.1	98.5
7	Foué 4H	45.2	1.0	8.2	7.4	0.3	7.9	27.5	2.1	0.3	0.1	100.0
8	Gatope 3B	29.1	0.9	8.8	7.0	0.1	6.4	44.5	1.9	0.3	0.1	99.3
9	Pointe de Pandope 3H	49.5	1.3	13.2	9.7	0.2	6.2	15.6	3.1	0.8	0.2	99.8
10	Maamat 4H	62.2	1.1	2.7	1.7	0.1	2.5	28.7	1.0	0.1	0.0	100.0
11	Pouébo 5B	90.4	0.3	3.6	2.0	0.1	0.6	1.5	0.8	0.3	0.0	99.6
12	Hienghène 4H	72.0	0.6	11.5	5.3	0.1	2.7	3.7	2.0	1.2	0.1	99.2
13	Poindimié 9B	85.7	0.2	3.3	3.0	0.0	2.7	4.3	0.6	0.2	0.0	100.1
14	Plage de Ouroué 3B	43.8	0.4	5.9	27.5	0.3	15.0	2.1	0.8	0.3	0.0	96.3
15	Prony 3H	13.8	0.3	10.7	59.4	2.3	3.7	0.2	0.6	0.2	0.0	91.2
16	Plum 4H	26.4	0.1	4.1	30.8	0.4	17.9	14.8	0.5	0.1	0.0	95.4
17	Ilot Maître 4B	0.0	0.0	0.2	0.1	0.0	5.8	92.7	0.4	0.1	0.1	99.3
18	Baie de Kuto 4B	0.0	0.0	0.1	0.1	0.0	6.0	92.4	0.2	0.0	0.2	99.1
19	Baie de Ouaméo 3B	0.0	0.0	0.3	0.0	0.0	0.6	97.1	0.3	0.0	0.0	98.2
20	Baie d'Upi 4B	1.6	0.0	0.3	0.2	0.0	1.6	93.4	0.6	0.1	0.1	98.0
21	Baie de Chateaubriand 3B	0.4	0.0	0.3	0.2	0.0	4.5	92.3	0.4	0.0	0.1	98.3
21	Baie de Chateaubriand 12H	0.7	0.1	0.7	0.8	0.0	4.4	89.9	0.4	0.0	0.1	97.3
22	Baie de Wadrilla 4B	0.5	0.0	0.4	0.5	0.0	2.8	93.5	0.5	0.1	0.2	98.3

Carbonate beaches are in roman, detrital beaches in *italics* and mixed ones in **bold**.

(3–13%) and Fe_2O_3 contents (1–59%). The Roche Percée (4), Pouébo (11) and Poindimié (13) beaches are rich in quartz, while Prony (15) and Plum (16) are remarkable for their high content of lateritic grains (Fe, Al). Pointe de Pandope (9), Hienghène (12) and Plage de

Table 6. *Maximum, minimum, mean and median MS values ($m^3\ kg^{-1}$) for the different beaches*

	Name	Minimum	Maximum	Mean	Median
2	Kuendu 2	1.97×10^{-9}	4.861×10^{-7}	1.08×10^{-7}	4.32×10^{-8}
6	Poé	6.69×10^{-9}	2.62×10^{-7}	2.88×10^{-8}	1.19×10^{-8}
17	Ilot Maitre	-1.90×10^{-9}	7.66×10^{-9}	5.73×10^{-11}	-1.05×10^{-9}
18	Baie de Kuto	-2.88×10^{-9}	1.30×10^{-8}	-5.16×10^{-10}	-1.90×10^{-9}
19	Baie de Ouaméo	9.74×10^{-10}	1.25×10^{-7}	1.57×10^{-8}	5.96×10^{-9}
20	Baie d'Upi	3.12×10^{-8}	1.82×10^{-7}	9.69×10^{-8}	9.12×10^{-8}
21	Baie de Chateaubriand	2.02×10^{-8}	2.11×10^{-6}	4.01×10^{-7}	1.13×10^{-7}
22	Baie de Wadrilla	-3.96×10^{-9}	2.27×10^{-8}	2.39×10^{-9}	6.21×10^{-10}
1	Anse de Kuendu	5.36×10^{-8}	2.88×10^{-7}	1.31×10^{-7}	1.05×10^{-7}
3	Kuendu 3	5.14×10^{-9}	2.81×10^{-7}	6.17×10^{-8}	4.08×10^{-8}
5	Baie des Tortues	8.52×10^{-8}	1.85×10^{-7}	1.31×10^{-7}	1.30×10^{-7}
7	Foué	4.42×10^{-7}	7.09×10^{-6}	3.22×10^{-6}	3.19×10^{-6}
8	Gatope	1.28×10^{-6}	3.06×10^{-6}	2.17×10^{-6}	2.21×10^{-6}
10	Maamat	5.59×10^{-10}	1.27×10^{-7}	3.27×10^{-8}	1.62×10^{-8}
4	Roche Percée	7.19×10^{-7}	2.44×10^{-6}	1.19×10^{-6}	9.26×10^{-7}
9	Pointe de Pandope	3.58×10^{-6}	6.48×10^{-6}	4.75×10^{-6}	4.63×10^{-6}
11	Pouébo	2.01×10^{-10}	4.85×10^{-7}	1.66×10^{-7}	8.25×10^{-8}
12	Hienghène	8.89×10^{-8}	1.34×10^{-7}	1.07×10^{-7}	1.08×10^{-7}
13	Poindimié	1.20×10^{-6}	1.98×10^{-5}	4.79×10^{-6}	3.19×10^{-6}
14	Plage de Ouroué	4.69×10^{-6}	7.61×10^{-6}	6.70×10^{-6}	6.93×10^{-6}
15	Prony	3.63×10^{-6}	7.14×10^{-6}	5.42×10^{-6}	6.09×10^{-6}
16	Plum	2.30×10^{-6}	8.19×10^{-6}	4.50×10^{-6}	4.16×10^{-6}

Carbonate beaches are in roman, detrital beaches in *italics* and mixed ones in **bold**.

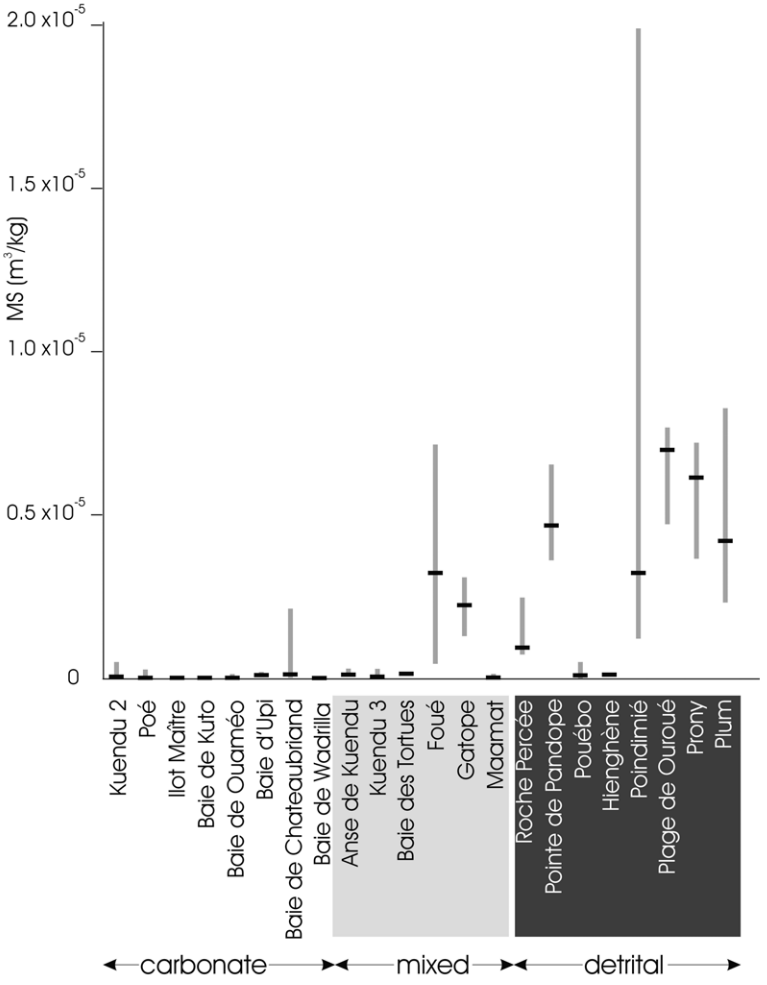

Fig. 8. Maximum, minimum and median MS values for the different beaches.

Ouroué (14) are highly mixed, with bioclasts, quartz grains and lateritic lithoclasts.

Magnetic susceptibility

All the samples (surface and 10 or 20 cm depth) were measured for MS. The main results are summarized in Table 6 and Figure 8. As for geochemical results, MS values vary significantly, from -4×10^{-9} to 2×10^{-5} $m^3\ kg^{-1}$. The lowest values are recorded from carbonate beaches – Kuendu (2), Poé (6), Ilot Maître (17), Baie de Kuto (18), Baie de Ouaméo (19), Baie d'Upi (20), Baie de Wadrilla (22) – and the highest, from detrital ones – Roche Percée (4), Pointe de Pandope (9), Poindimié (13), Plage de Ouroué (14), Prony (15) and Plum (16). Pouébo (11) and Hienghène (12) are detrital beaches with low values of MS, probably owing to their high quartz content. Two carbonate beaches are distinguished by their relatively high MS values: Baie de Chateaubriand (21) and Baie d'Upi (20).

The comparison of MS between loose sediment and corresponding beachrocks (Fig. 9) shows that the latter have significantly lower values, by several orders of magnitude. The exception is Ilot Maître, which actually corresponds to a hardground rather than a beachrock.

Discussion

The aim of this section is to question the relationship between MS and the other characteristics of the sediments described above. Compared with ancient

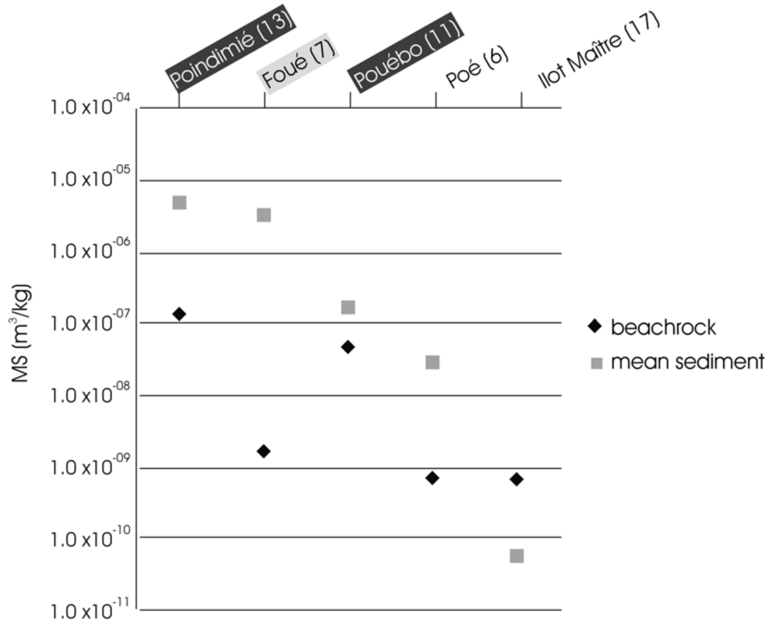

Fig. 9. Comparison of MS values of beachrocks and equivalent loose sediment.

sediments, recent ones are supposed to be less complex. Actually, ancient rocks suffer from frequent post-depositional transformations (from early diagenesis to metamorphism) that can heavily affect the original MS signal (e.g. McCabe & Elmore 1989; Elmore *et al.* 2001; Zegers *et al.* 2003; Devleeschouwer *et al.* 2010; Riquier *et al.* 2010; Da Silva *et al.* 2012, 2013) and their primary environmental setting is not always well constrained. The main advantages of the studied samples are that they are recently deposited and little affected by diagenesis, and that they are a direct reflection of the environmental setting. Assuming that the primary origin of the MS signal is preserved, one of the strongest statements made when using this signal for correlation purposes or for palaeoenvironmental reconstructions is that MS is proportional to detrital content and is a reflection of eustasy through changes in river base level (Crick *et al.* 1997). This study shows that even in geographically close time-equivalent settings of a carbonate platform, MS values may be highly different: compare for example Baie des Tortues (5), 1.31×10^{-7}, with the 6 km distant Poé beach (6), 2.88×10^{-8}. This reflects the unequal distribution of the MS carriers in the lagoon. Even in places where no rivers flow into the lagoon (Gatope, 8), marine erosion of cliffs and beach outcrops may deliver MS carriers to the sediment.

An inverse relationship between carbonate content and detrital supply is observed, as seen by the negative correlation between CaO content and magnetic susceptiblity. The MS/CaO diagram (Fig. 10a) shows the three beach types already defined. Carbonate beaches have a low MS and high CaO content, detrital beaches are characterized by variable but often high MS and low CaO and mixed beaches show intermediate results. This relation was already observed in recent lake sediments by Kirby *et al.* (2007) and ancient rocks by Ellwood *et al.* (2000). Detrital and mixed beaches with low MS values correspond to quartz-rich (Pouébo, 11) or carbonate-rich (Anse de Kuendu, 1) sands. The only carbonate beaches with a relatively high MS signal (Baie de Chateaubriand, 21) or with a highly variable MS signal (Baie d'Upi, 20) will be further discussed below.

When considering the relationship between MS and well-known geochemical proxies of detrital input such as Si, Ti and Al (Tribovillard *et al.* 2006; Calvert & Pedersen 2007; Riquier *et al.* 2010), only weak correlation is observed (Fig. 10b and c). This clearly questions the use of MS as detrital proxy on its own, without testing its relationship with Si, Ti or Al. However, other links between MS and the geochemical content are interesting, especially with Fe and Mn (Fig. 10d and e). As already proposed by Dessai *et al.* (2009) for Indian recent estuarine sediment, a fairly good positive correlation ($r^2 = 0.85$) between MS and Fe or Mn is detected, especially when removing the samples from Plum (16) and Prony (15) (Fig. 10f).

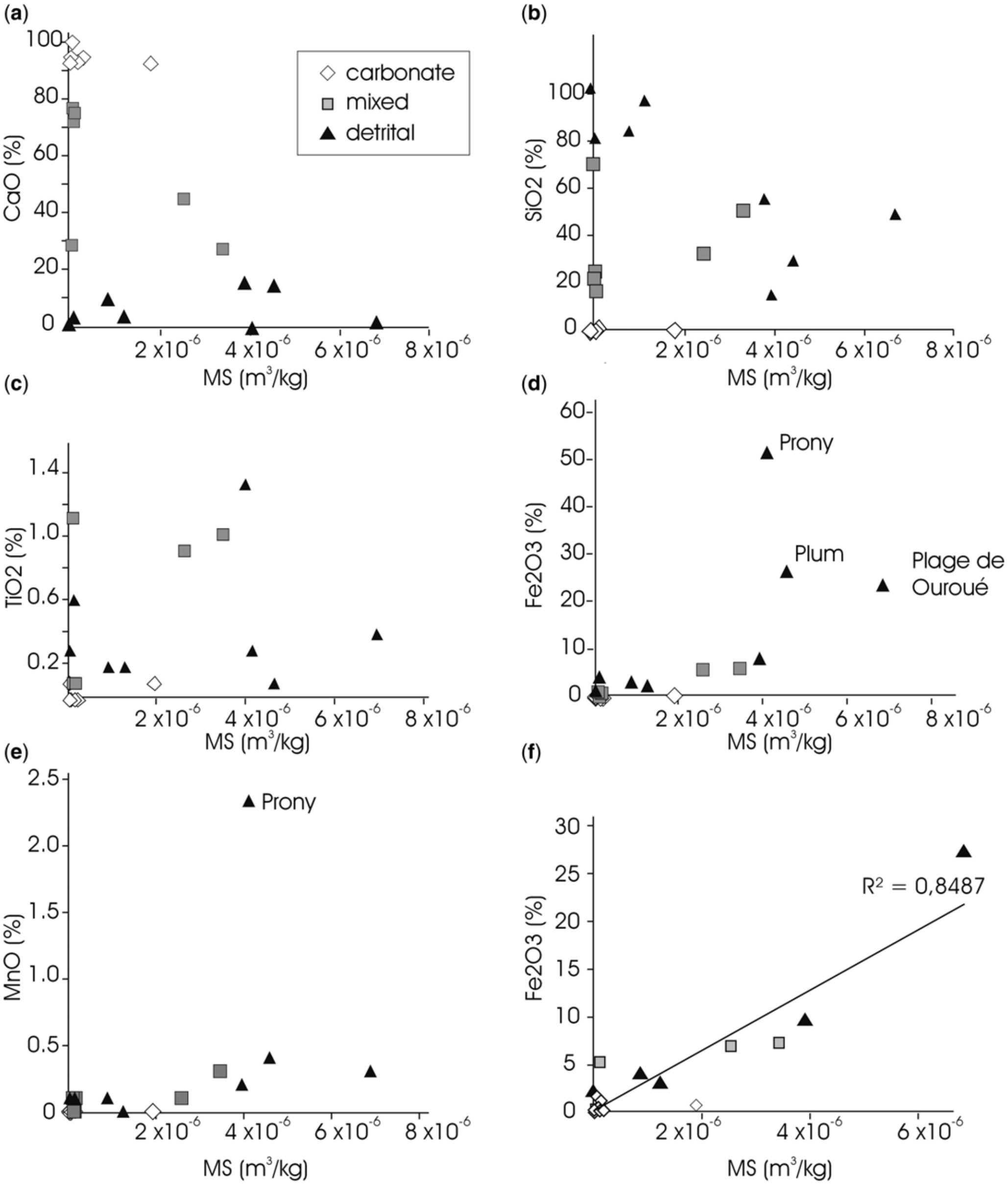

Fig. 10. MS v. CaO (**a**), SiO_2 (**b**), TiO_2 (**c**), Fe_2O_3 (**d**) and MnO (**e**). (**f**) Correlation graph for MS and Fe_2O_3.

Plum and Prony have an anomalous Fe_2O_3/MS value, probably owing to their very high content in fragments of lateritic crust. The correlation with Mn content is also relevant ($r^2 = 0.80$) and suggests that the main MS carriers are ferromagnetic iron oxides, here supplied by marine or continental erosion of magmatic rocks.

The next question concerns the relationship between surface and subsurface sediment. In shallow-water carbonate sediments, primary MS seems to be related mainly to bacterial magnetite (Bahamas; McNeill *et al.* 1988) and its preservation decreases with depth (Queensland plateau; McNeill 1993). Hladil *et al.* (2003, 2004) reported MS anomalies in subsurface Late Pleistocene carbonates from the Bahamas, but it was related to the development of microbial magnetite during exposure and soil development. Throughout our study, all surface

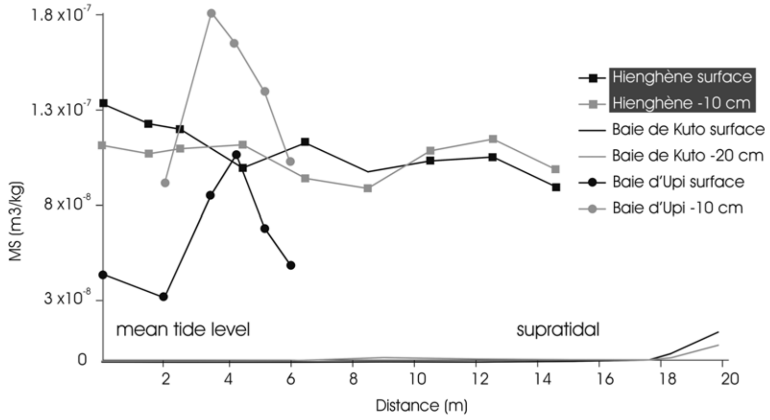

Fig. 11. Examples of MS surface and subsurface profiles for detrital and carbonate beaches.

samples were complemented by sediment grabbed at 10 or 20 cm depth, depending the thickness of the loose sediment blanket. When compared, all of the surface/subsurface MS profiles are strikingly similar, whatever the type of beach or the MS magnitude order. Figure 11 shows an example of this relationship for carbonate and detrital beaches: among others, the Baie d'Upi (20) profile is remarkable in the fact that strong MS peaks appear at the same place in the two sets of samples. This observation shows that little change in MS occurs in the first 20 cm, but usually the grain size of the sediment is too coarse to allow the development of magnetite producing bacteria.

Grain size is an important sedimentological parameter. It is strongly related to beach morphology through wave energy. Beaches exposed to rough waves are steeper and have a profile characterized by a micro-cliff located near the base of the supratidal zone. Sediments are coarse, fine-grained

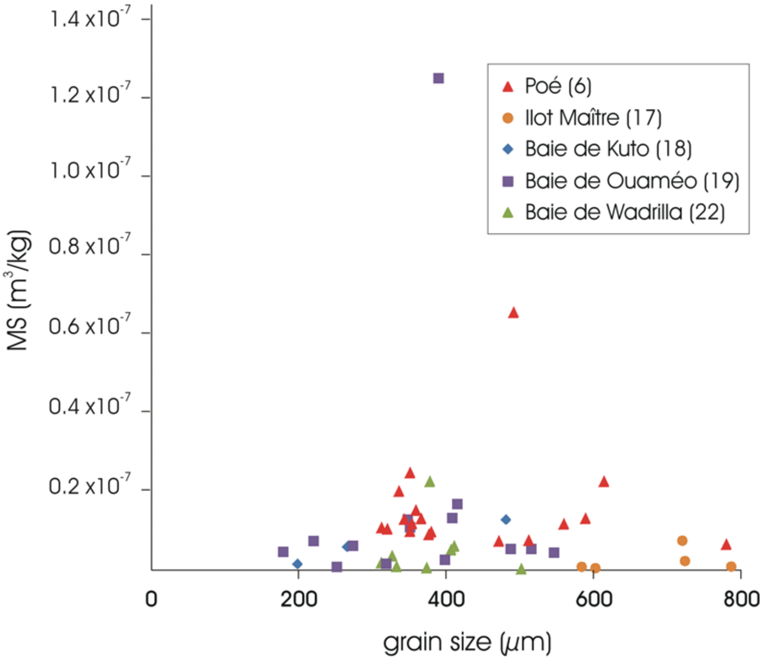

Fig. 12. MS v. grain size for carbonate beaches.

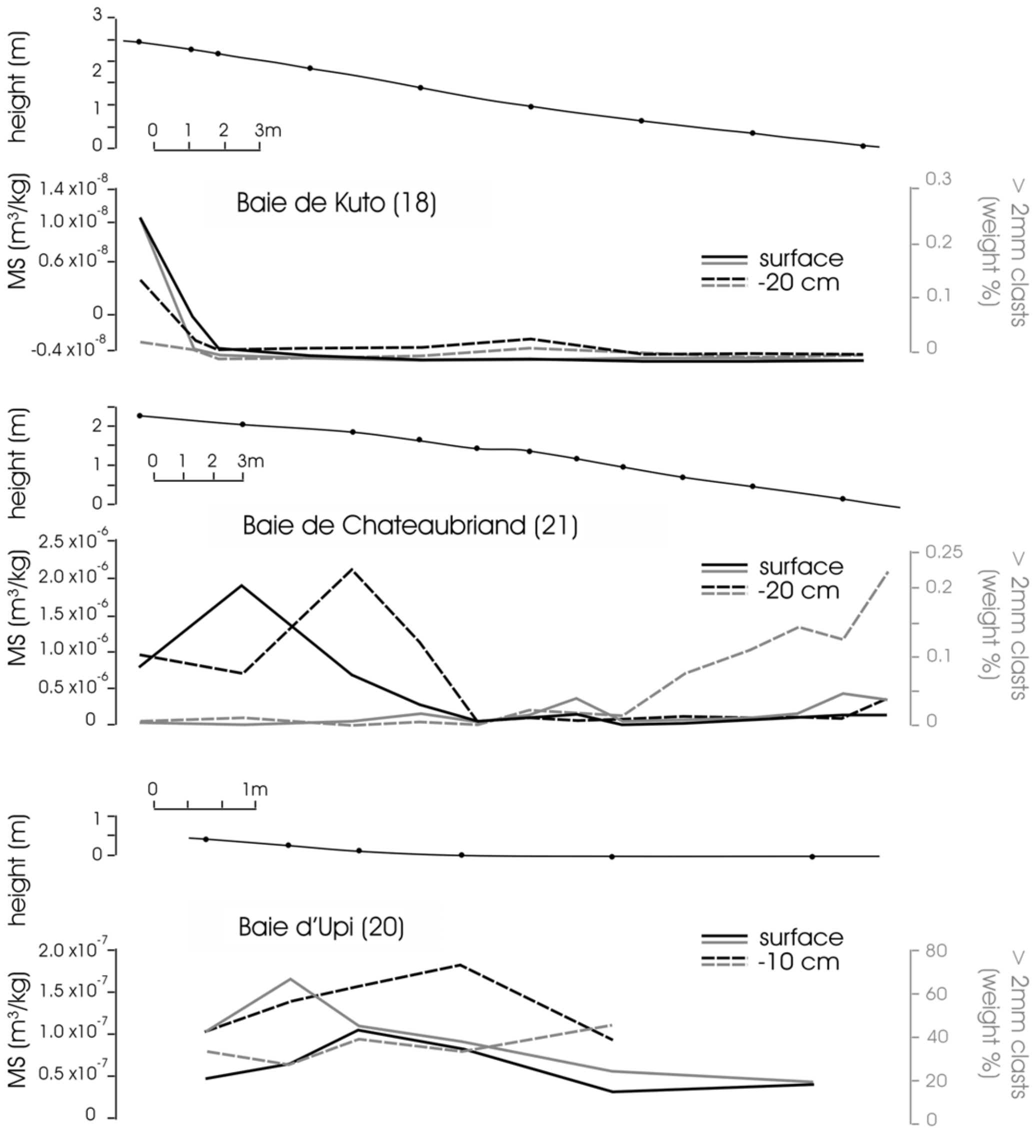

Fig. 13. MS values and coarse clasts content along the profiles of Baie de Kuto (18), Baie de Chateaubriand (21) and Baie d'Upi (20) beaches.

particles are driven offshore and erosion is important during storms. On the other hand, beaches with low-energy waves have a flatter, longer profile with finer-grained sediments. Erosion is weak and littoral accretion dominates (Davidson-Arnott 2010). Coarser grains and heavy minerals are carried 10–30 cm below the finer-grained superficial sediment blanket (Salomon 2008). New Caledonia is protected by a reef barrier and wave energy is commonly low except were reefs are interrupted. Grain-size studies on beaches and lagoon have shown that sediment sorting is relatively weak and that accretion is dominant (Godart *et al.* 1985). Our comparison between surface and subsurface samples confirms that sediment is commonly coarser-grained below 10 cm depth, excepted for the Kuendu beaches (2, 3), which are characterized by coarser-grained surface sediments topping finer-grained ones. A relation between MS and grain size was previously proposed for recent sediments by Thompson & Morton (1979), for Pleistocene facies by Gautam *et al.* (2009) and for Devonian

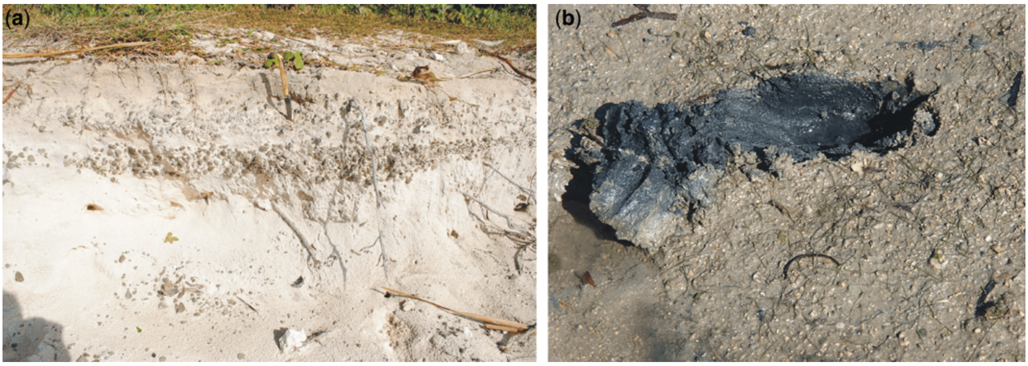

Fig. 14. (**a**) Pumice layers in the erosion cliff bordering the supratidal zone in Lifou (Baie de Chateaubriand) (21). (**b**) Footprint showing the reducing sediment below the surface of the sediment in Baie d'Upi (20) (Ile des Pins).

rocks by Da Silva *et al.* (2009*a*), who show that water agitation during sedimentation can prevent magnetic particles from settling and that coarse textures have lower MS than finer ones. However, on the contrary, Dessai *et al.* (2009) observed a positive link between MS and grain size in recent detrital estuary sediments.

In New Caledonia, the relationship between MS and grain-size remains unclear (Fig. 12), despite a slight tendency towards a positive correlation. This may be due to the important and variable supply of skeletal carbonates from the reef barrier and the relatively low sorting effect of waves and marine currents in the lagoon. However, several carbonate beaches show some positive relation between MS and grain size (percentage gravel; see Baie de Kuto, 18, for example; Fig. 13a). Moreover, when the subsurface sediment is coarser than the surface sediment, the MS signal is significantly higher. Other beaches, like Baie de Chateaubriand (21) (Fig. 13b) or Baie d'Upi (20) (Fig. 13c) have different characteristics. These two beaches were already noted for their high MS (see above).

The Baie de Chateaubriand (21) anomaly with high MS values and low grain size in the upper part of the intertidal zone is probably related to the presence of pumice, whose well-defined layers were observed in the cliff bordering the supratidal zone (Fig. 14a). This was confirmed by a Fe–Mg anomaly in the high MS samples (cf. Table 5). The other anomaly concerns the subsurface sediments from Baie d'Upi (20) and seems to be due to the reducing conditions affecting all the fine-grained sediments below the 1 cm-thick surface carpet (Fig. 14b; Hladil *et al.* 2003).

The relationship between low MS beachrocks and their high MS loose sediment equivalent is very interesting. Beachrocks are characterized by rapid precipitation of different types of carbonate cements (Purser 1980). With this additional supply of low-MS diamagnetic material, the total MS signal of the sample must be lower than of the loose sediment. The scale of the difference (Fig. 9), however, remains surprising and must be further questioned.

Conclusions

Following the integrated MS and geochemical analyses, three types of beaches were identified: carbonate beaches are rich in bioclasts (>95%) and have a CaO content higher than 90%. Their mean MS is commonly very low, between -5×10^{-10} and 4×10^{-7} m^3 kg^{-1}. These values are consistent with published values for Palaeozoic carbonate platforms (Bertola *et al.* 2013). Detrital beaches may include up to 30% bioclasts but have low CaO (<15%). Depending from the nature of the detrital supply, these beaches are rich in Si, Al, Fe or Mg. Their mean MS signal is high, varying between 1×10^{-7} and 7×10^{-6} m^3 kg^{-1}. The mixed beaches have a CaO concentration higher than 30% and a variable bioclastic content. Some of these beaches are close to a reef, but the marine erosion of magmatic or metamorphic rocks delivers a plentiful supply of detritus that balances the carbonate production. Others are influenced by fluvial delivery of various detrital material, but are far enough from the river mouths to be also supplied by bioclasts. Their mean MS is variable. The influence of detrital input on the MS signal is best reflected by the positive Fe and Mn/MS correlation, suggesting that ferromagnetic minerals make the bulk of the MS signature of the sediments.

Surface and subsurface MS profiles are strikingly similar, ruling out the hypothesis of an early diagenesis affecting MS carriers. In contrast, beachrocks show a strongly reduced MS signal, probably related to the precipitation of variable amounts of carbonate cement.

There is no link between the nature of the beaches and the grain size of the sediments. Close vicinity to a reef or outcrops is reflected by a large amount of coarse bioclasts or lithoclasts in the sediment. Without the influence of strong waves or marine currents, New Caledonia's protected beaches are poorly sorted and littoral accretion is dominant, with deposition of relatively fine-grained sediment as a surface blanket in the intertidal zone. The MS signal of carbonates is locally linked to grain size: the coarser the sediment, the higher the MS signal. Two noteworthy exceptions suggest that the MS signal may also be influenced by an exceptional supply of volcanic ash and by the presence of a subsurface reducing layer.

This paper is part of the IGCP580 international program 'Application of magnetic susceptibility as a palaeoclimatic proxy on Palaeozoic sedimentary rocks and characterization of the magnetic signal'. We thank J. Vander Auwera (Université de Liège) for access and help on the geochemical measurements and M. Allenbach, P. Chaillan, S. Lemouellic, N. Selmaoui-Folcher, D. Cluzel, N. Folcher and V. Lignier (Université de Nouméa) for support during our stay in New Caledonia. M. Whalen and S. Spassov are gratefully acknowledge for their precise and interesting comments on this text.

References

Audet, M. A. 2008. *Le massif du Koniambo, Nouvelle-Calédonie. Formation et obduction d'un complexe ophiolitique du type SSZ. Enrichissement en nickel, cobalt et scandium dans les profils résiduels*. Thèse de doctorat, Université du Québec et Université de la Nouvelle-Calédonie, 327 pp.

Bábek, O., Kalvoda, J., Cossey, P., Šimíek, D., Devuyst, F-X. & Hargreaves, S. 2013. Facies and petrophysical signature of the Tournaisian/Viséan (Lower Carboniferous) sea-level cycle in carbonate ramp to basinal settings of the Wales-Brabant massif, British Isles. *Sedimentary Geology*, **284–285**, 197–213.

Baltzer, F. & Trescases, J. J. 1971. Erosion, transport et sédimentation liés aux cyclones tropicaux dans les massifs d'ultrabasites de Nouvelle-Calédonie. Première approche du bilan général d'altération, de l'érosion et de la sédimentation sur péridotite en zone tropicale. *Cahiers ORSTOM Géologie*, **3**, 221–244.

Bender, V. B., Hanebuth, T. J. J., Mena, A., Baumann, K. H., Francés, G. & von Dobeneck, T. 2012. Control of sediment supply, palaeoceanography and morphology on late Quaternary sediment dynamics at the Galician continental slope. *Geo-Marine Letters*, **32**, 313–335.

Bertola, C., Boulvain, F., Da Silva, A. C. & Poty, E. 2013. Sedimentology and magnetic susceptibility of Mississippian (Tournaisian) carbonate sections in Belgium. *Bulletin of Geosciences*, **88**, 69–82.

Blatt, H., Middleton, G. & Murray, R. 1972. *Origin of Sedimentary Rocks*. Prentice Hall, Englewood Cliffs, NJ.

Bloemendal, J., Tauxe, L., Valet, J. P. & Party, S. S. 1988. High-resolution, whole-core magnetic susceptibility logs from leg 108. *In*: Ruddiman, W., Sarnthein, M., Baldauf, J. et al. (eds) *Proceedings ODP, Initial Reports*. Ocean Drilling Program, Texas A & M University, College Station, TX, **18**, 1005–1013.

Borradaile, G. J., Chow, N. & Werner, T. 1993. Magnetic hysteresis of limestones: facies control? *Physics of the Earth and Planetary Interiors*, **76**, 241–252.

Boulila, S., Galbrun, B., Hinno, L. A. & Collin, P. Y. 2008. High-resolution cyclostratigraphic analysis from magnetic susceptibility in a Lower Kimmeridgian (Upper Jurassic) marl and limestone succession (La Méouge, Vocontian Basin, France). *Sedimentary Geology*, **203**, 54–63.

Boulvain, F., Da Silva, A. C., Mabille, C., Hladil, J., Gersl, M., Koptikova, L. & Schnabl, P. 2010. Magnetic susceptibility correlation of km-thick Eifelian–Frasnian sections (Ardennes and Moravia). *Geologica Belgica*, **13**, 309–318.

Calvert, S. E. & Pedersen, T. F. 2007. Elemental proxies for palaeoclimatic and palaeoceanographic variability in marine sediments: interpretation and application (Chapter 14). *In*: Hillaire-Marcel, C. & De Vernal, A. (eds) *Developments in Marine Geology*. Elsevier, Oxford, 567–644.

Chevillon, C. 1997. Sédimentologie descriptive des fonds meubles du lagon de la côte Est de la Nouvelle-Calédonie. In: Richer de Forges, B. (ed.) *Les fonds meubles des lagons de Nouvelle-Calédonie (Sédimentologie et Benthos)*. ORSTOM, Etudes & Thèses, Paris, France, **3**, 7–30.

Chevillon, C. 2013. Le lagon sud-ouest de la Grande-Terre. Géomorphologie, sédimentologie. In: Bonvallo, J., Ga, J-C. & Haber, E. (eds) *Atlas de la Nouvelle-Calédonie*. IRD editions, Paris, France, 35–37.

Clavier, J. & Garrigue, C. 1999. Annual sediment primary production and respiration in a large coral reef lagoon (SW New Caledonia). *Marine Ecology Progress Series*, **191**, 79–89.

Cluzel, D. 2006. *Synthèse géologique de la Nouvelle-Calédonie et de sa zone économique exclusive*. Rapport de synthèse de la convention ISTO-IFREMER, programme EXTRAPLAC.

Cluzel, D., Maurizot, P., Collot, J. & Sevin, B. 2012. An outline of geology of New-Caledonia; from Permian-Mesozoic Southeast Gondwanaland active margin to Cenozoic obduction and supergene evolution. *Episodes*, **35**, 1–15.

Crick, R. E., Ellwood, B. B., El Hassani, A., Feist, R. & Hladil, J. 1997. Magnetosusceptibility event and cyclostratigraphy (MSEC) of the Eifelian–Givetian GSSP and associated boundary sequences in North Africa and Europe. *Episodes*, **20**, 167–175.

Crick, R. E., Ellwood, B. B., Hladil, J., Hassani, A. E., Hrouda, F. & Chlupac, I. 2001. Magnetostratigraphy susceptibility of the Pridolian–Lochkovian (Silurian–Devonian) GSSP (Klonk, Czech Republic) and coeval sequence in Anti-Atlas Morocco. *Palaeogeography, Palaeoclimatolology, Palaeoecology*, **167**, 73-I(X).

Da Silva, A. C. & Boulvain, F. 2006. Upper Devonian carbonate platform correlations and sea level variations recorded in magnetic susceptibility. *Palaeogeography, Palaeoclimatology, Palaeoecology*, **240**, 373–388.

Da Silva, A. C. & Boulvain, F. 2012. Multi-faceted approach for basin evolution reconstitution: analysis of the Devonian platform from Belgium. *Basin Research*, **24**, 338–356.

Da Silva, A. C., Mabille, C. & Boulvain, F. 2009*a*. Influence of sedimentary setting on the use of magnetic susceptibility: examples from the Devonian of Belgium. *Sedimentology*, **56**, 1292–1306.

Da Silva, A. C., Potma, K., Weissenberger, J. A. W., Whalen, M. T., Humblet, M., Mabille, C. & Boulvain, F. 2009*b*. Magnetic susceptibility evolution and sedimentary environments on carbonate platform sediments and atolls, comparison of the Frasnian from Belgium and Alberta, Canada. *Sedimentary Geology*, **214**, 3–18.

Da Silva, A. C., Dekkers, M., Mabille, C. & Boulvain, F. 2012. Magnetic signal and its relationship with paleoenvironments and diagenesis – examples from the Devonian carbonates of Belgium. *Studia Geophysica & Geodaedica*, **56**, 677–704.

Da Silva, A. C., De Vleeschouwer, D. *et al.* 2013. Magnetic susceptibility as a high-resolution correlation tool and as a climatic proxy in Palaeozoic rocks – merits and pitfalls: examples from the Devonian in Belgium. *Marine and Petroleum Geology*, **46**, 173–189.

Davidson-Arnott, R. 2010. *Introduction to Coastal Processes and Geomorphology*. Cambridge University Press, Cambridge.

Debacker, T. N., Sintubin, M. & Robion, P. 2010. On the use of magnetic techniques for stratigraphic purposes: examples from the lower palaeozoic anglo-brabant deformation belt (Belgium). *Geologica Belgica*, **13**, 333–350.

Debenay, J-P. 2013. *A Guide to 1000 Foraminifera from Southwestern Pacific: New Caledonia*. IRD editions, Paris, France.

Dessai, D. V. G., Nayak, G. N. & Basavaiah, N. 2009. Grain size, geochemistry, magnetic susceptibility: proxies in identifying sources and factors controlling distribution of metals in a tropical estuary, India. *Estuarine, Coastal and Shelf Science*, **85**, 307–318.

Devleeschouwer, X. 1999. *La transition Frasnien-Famennien (Dévonien Supérieur) en Europe: Sédimentologie, stratigraphie séquentielle et susceptibilité magnétique*. PhD (inédite), Université Libre de Bruxelles, Belgium.

Devleeschouwer, X., Petitclerc, E., Spassov, S. & Préat, A. 2010. The Givetian–Frasnian boundary at Nismes parastratotype (Belgium): the magnetic susceptibility signal controlled by ferromagnetic minerals. *In*: Da Silva, A. C. & Boulvain, F. (eds) *Magnetic Susceptibility, Correlations and Palaeozoic Environments*. Geologica Belgica, **13**, 351–366.

Donghuai, S., Zhisheng, A., Shaw, J., Bloemendal, J. & Youbin, S. 1998. Magnetostratigraphy and palaeoclimatic significance of Late Tertiary aeolian sequences in the Chinese Loess Plateau. *Geophysical Journal International*, **134**, 207–212.

Dugas, F. & Debenay, J.-P. 1980. Sédimentologie: sud-ouest du Lagon: [planche 8]. *In*: *Atlas de la Nouvelle-Calédonie/carte établie par le service cartographique de l'ORSTOM*, 1:200000 (E 165°55′ 00″–E 166°53′ 00″/S 21°53′ 00″–S 22°35′ 00″).

Dupont, J. & Daniel, J. 1981. La Nouvelle-Calédonie et ses dépendances: carte bathymétrique détaillée. *In*: Sautter, G., Huetz de Lemps, A. & Lerand, M. (eds) *Atlas de la Nouvelle-Calédonie et de ses dépendances*. Map scale 1:3,640,000 (E 157–E 174/S17–S 24). ORSTOM, Paris, France.

Ellwood, B. B., Crick, R. E. & El Hassani, A. 1999. Magnetosusceptibility event and cyclostratigraphy (MSEC) method used in geological correlation of Devonian rocks from Anti-Atlas Morocco. *American Association of Petroleum Geologists Bulletin*, **83**, 1119–1134.

Ellwood, B. B., Crick, R. E., El Hassani, A., Benoist, S. L. & Young, R. H. 2000. Magnetosusceptibility event and cyclostratigraphy method applied to marine rocks: detrital input v. carbonate productivity. *Geology*, **28**, 1135–1138.

Elmore, R. D., Kelley, J., Evans, M. & Lewchuk, M. T. 2001. Remagnetization and orogenic fluids: testing the hypothesis in the central Appalachians. *Geophysical Journal International*, **144**, 568–576.

Folk, R. L. & Ward, W. C. 1957. Brazos river bar: a study in the significance of grain size parameters. *Journal of Sedimentary Petrology*, **27**, 514–529.

Gautam, P., Sakai, T., Paudayal, K. M., Bhandari, S., Gyawali, B. R., Gautam, C. M. & Rijal, M. L. 2009. Magnetism and granulometry of Pleistocene sediments of Dhapasi section, Kathmandu (Nepal): implications for depositional age and palaeoenvironment. *Bulletin of the Department of Geology, Tribhuvan University, Kathmandu, Nepal*, **12**, 17–28.

Godart, A., Vanney, J.-R., Verger, F. & Carre, F. 1985. *André Guilcher, Géographie de la mer*. Edition Paradigme Caen, France.

Grabowski, J. & Pszczoikowski, A. 2006. Magneto- and biostratigraphy of the Tithonian and Berriasian pelagic sediments in the Tatra Mountains (central Western Carpathians, Poland): sedimentary and rock magnetic changes at the Jurassic/Cretaceous boundary. *Cretaceous Research*, **27**, 398–417.

Grenz, C., le Borgne, R., Fichez, R. & Torréton, J-P. 2010. Tropical lagoon multidisciplinary investigations: An overview of the PNEC New Caledonia pilot site. *Marine Pollution Bulletin*, **61**, 267–268.

Hladil, J. 2002. Geophysical records of dispersed weathering products on the Frasnian carbonate platform and early Famennian ramps in Moravia, Czech Republic: proxies for eustasy and palaeoclimate. *Palaeogeography, Palaeoclimatology, Palaeoecology*, **181**, 213–250.

Hladil, J., Bosak, P., Slavik, L., Carew, J. L., Mylroie, J. E. & Gersl, M. 2003. Early diagenetic origin and persistence of gamma-ray and magnetosusceptibility patterns in platform carbonates: comparison of Devonian and Quaternary sections. *Physics and Chemistry of the Earth*, **28**, 719–727.

Hladil, J., Carew, J. L. *et al.* 2004. Anomalous magnetic susceptibility values and traces of subsurface microbial activity in carbonate banks on San Salvador Island, Bahamas. *Facies*, **50**, 161–182.

Hladil, J., Gersl, M., Strnad, L., Frana, J., Langrova, A. & Spisiak, J. 2006. Stratigraphic variation of complex impurities in platform limestones and possible significance of atmospheric dust: a study with emphasis on gamma-ray spectrometry and magnetic susceptibility outcrop logging (Eifelian–Frasnian, Moravia, Czech Republic). *International Journal of Earth Sciences*, **95**, 703–723.

Hladil, J., Koptikova, L. *et al.* 2009. Early Middle Frasnian platform reef strata in the Moravian Karst interpreted as recording the atmospheric dust changes: the key to understanding perturbations in the *punctata* conodont Zone. *Bulletin of Geosciences*, **84**, 75–106.

Hladil, J., Vondra, M., Cejchan, P., Vich, R., Koptikova, L. & Slavik, L. 2010. The dynamic time-warping approach to comparison of magnetic-susceptibility logs and application to Lower Devonian calciturbidites (Prague Synform, Bohemian Massif). *Geologica Belgica*, **13**, 385–406.

Illing, L. V. 1954. Bahaman calcareous sands. *American Association of Petroleum Geologists Bulletin*, **38**, 1–95.

Kirby, M. E., Lund, S. P., Anderson, M. A. & Bird, B. W. 2007. Insolation forcing of Holocene climate change in Southern California: a sediment study from Lake Elsinore. *Journal of Palaeolimnology*, **38**, 395–417.

Koptíková, L., Bábek, O., Hladil, J., Kalvoda, J. & Slavík, L. 2010. Stratigraphic significance and resolution of spectral reflectance logs in Lower Devonian carbonates of the Barrandian area, Czech Republic; a correlation with magnetic susceptibility and gamma-ray logs. *Sedimentary Geology*, **225**, 83–98.

Lambert, B. & Roux, M. 1991. L'environnement carbonaté bathyal en Nouvelle-Calédonie (programme ENVIMARGES). *Documents et travaux, Institut géologique Albert-de-Lapparent*, **15**, 213.

Mabille, C. & Boulvain, F. 2007. Sedimentology and magnetic susceptibility of the Upper Eifelian – Lower Givetian (Middle Devonian) in southwestern Belgium: insights into carbonate platform initiation. *In*: Álvaro, J. J., Aretz, M., Boulvain, F., Munnecke, A., Vachard, D. & Vennin, E. (eds) *Palaeozoic Reefs and Bioaccumulations: Climatic and Evolutionary Controls*. Geological Society, London, Special Publications, **275**, 109–124.

McCabe, C. & Elmore, R. D. 1989. The occurrence and origin of late Palaeozoic remagnetizations in the sedimentary rocks of North America. *Reviews of Geophysics*, **27**, 471–494.

McNeill, D. F. 1993. A review and comparison of carbonate rock magnetization: Leg 133, Queensland Plateau, Australia. *In*: McKenzie, J. A., Davies, P. J. & Palmer-Julson, A. (eds) *Proceedings ODP, Scientific Results*. Ocean Drilling Program, Texas A & M University, College Station, TX, **133**, 749–753.

McNeill, D. F., Ginsburg, R. N., Chang, S. B. R. & Kirschvink, J. L. 1988. Magnetostratigraphic dating of shallow-water carbonates from San Salvador, Bahamas. *Geology*, **16**, 8–12.

Marchand, C., Allenbach, M. & Lallier-Vergès, E. 2010. Relationships between heavy metals distribution and organic matter cycling in mangrove sediments (Conception Bay, New Caledonia). *Geoderma*, **160**, 444–456.

Michalík, J., Lintnerová, O. *et al.* 2013. Palaeoenvironments during the Rhaetian transgression and the colonization history of marine biota in the Fatric Unit (Western Carpathians). *Geologica Carpathica*, **64**, 39–62.

Montaggioni, L. F., Cabioch, G., Thouveny, N., Frank, N., Sato, T. & Sémah, A-M. 2011. Revisiting the Quaternary development history of the Western New Caledonian shelf system: from ramp to barrier reef. *Marine Geology*, **280**, 57–75.

Ouillon, S., Douillet, P. *et al.* 2010. Circulation and suspended sediment transport in a coral reef lagoon: the south-west lagoon of New Caledonia. *Marine Pollution Bulletin*, **61**, 269–296.

Paris, J-P. 1981. *Géologie de la Nouvelle-Calédonie: un essai de synthèse (Mémoire pour servir de notice explicative à la carte géologique de Nouvelle-Calédonie à l'échelle du 1/200 000)*. Mémoire du BRGM, **113**. BRGM, Orléans, France.

Purser, B. H. 1980. *Sédimentation et diagenèse des carbonates néritiques récents (Tome 1)*. Technip, Paris, France.

Riquier, L., Averbuch, O., Devleeschouwer, X. & Tribovillard, N. 2010. Diagenetic v. detrital origin of the magnetic susceptibility variations in some carbonate Frasnian-Famennian boundary sections from Northern Africa and Western Europe: implications for palaeoenvironmental reconstructions. *International Journal of Earth Sciences*, **99**, S57–S73.

Rochette, P. 1987. Metamorphic control of the magnetic mineralogy of black shales in the Swiss Alps: toward the use of 'magnetic isogrades'. *Earth & Planetary Sciences Letters*, **84**, 446–456.

Salomon, J.-N. 2008. *Géomorphologie sous-marine et littorale*. Presses universitaires de Bordeaux, France.

Spahn, Z. P., Kodama, K. P. & Preto, N. 2013. High-resolution estimate for the depositional duration of the Triassic Latemar Platform: a new magnetostratigraphy and magnetic susceptibility cyclostratigraphy from basinal sediments at Rio Sacuz, Italy, *Geochemistry Geophysics Geosystems*, **14**, 1245–1257.

Tang, Y., Jia, J. & Xie, X. 2003. Record of magnetic properties in Quaternary loess and its palaeoclimatic significance: a brief review. *Quaternary International*, **108**, 33–50.

Tercinier, G. 1962. *Les sols de la Nouvelle-Calédonie*. Cahiers ORSTOM pédologie, **1**, 1–54.

Thompson, R. & Morton, D. J. 1979. Magnetic susceptibility and particle size distribution in recent sediments of the Loch Lomond drainage basin. *Scotland Journal of Sedimentary Petrology*, **49**, 801–812.

Tribovillard, N., Algeo, T. J., Lyons, T. & Riboulleau, A. 2006. Trace metals as palaeoredox and palaeoproductivity proxies: an update. *Chemical Geology*, **232**, 12–32.

Vacek, F. 2011. Palaeoclimatic event at the Lochkovian–Pragian boundary recorded in magnetic susceptibility and gamma-ray spectrometry (Prague Synclinorium, Czech Republic). *Bulletin of Geosciences*, **86**, 259–268.

VIRLY, S. 2008. *Atlas des mangroves de la Nouvelle-Calédonie*. ZoNéCo, IRD-ORSTOM, Paris, France.

WHALEN, M. T. & DAY, J. E. 2008. Magnetic susceptibility, biostratigraphy, and sequence stratigraphy: insights into Devonian carbonate platform development and basin infilling, Western Alberta. *In*: LUKASIK, J. & SIMO, J. A. (eds) *Papers on Phanerozoic Reef Carbonates in Honor of Wolfgang Schlager*. SEPM (Society for Sedimentary Geology), Tulsa, OK, Special Publications, **89**, 291–314.

ZEGERS, T. E., DEKKERS, M. J. & BAILY, S. 2003. Late Carboniferous to Permian remagnetization of Devonian limestones in the Ardennes: role of temperature, fluids, and deformation. *Journal of Geophysical Research*, **108**, 5/1–5/19.